Preparation of Chloramphenicol/Amino Acid Combinations Exhibiting Enhanced Dissolution Rates and Reduced Drug-Induced Oxidative Stress

Vanesa B. Sterren, Virginia Aiassa, Claudia Garnero, Yamila Garro Linck, Ana K. Chattah, Gustavo A. Monti, Marcela R. Longhi, et al.

AAPS PharmSciTech
An Official Journal of the American Association of Pharmaceutical Scientists

e-ISSN 1530-9932

AAPS PharmSciTech
DOI 10.1208/s12249-017-0775-4

Springer

AAPS PharmSciTech (© 2017)
DOI: 10.1208/s12249-017-0775-4

Research Article

Preparation of Chloramphenicol/Amino Acid Combinations Exhibiting Enhanced Dissolution Rates and Reduced Drug-Induced Oxidative Stress

Vanesa B. Sterren,[1] Virginia Aiassa,[1] Claudia Garnero,[1] Yamila Garro Linck,[2] Ana K. Chattah,[2] Gustavo A. Monti,[2] Marcela R. Longhi,[1] and Ariana Zoppi[1,3]

Received 13 January 2017; accepted 3 April 2017

Abstract. Chloramphenicol is an old antibiotic agent that is re-emerging as a valuable alternative for the treatment of multidrug-resistant pathogens. However, it exhibits suboptimal biopharmaceutical properties and toxicity profiles. In this work, chloramphenicol was combined with essential amino acids (arginine, cysteine, glycine, and leucine) with the aim of improving its dissolution rate and reduce its toxicity towards leukocytes. The chloramphenicol/amino acid solid samples were prepared by freeze-drying method and characterized in the solid state by using Fourier transform infrared spectroscopy, powder X-ray diffraction, differential scanning calorimetry, scanning electron microscopy, and solid-state nuclear magnetic resonance. The dissolution properties, antimicrobial activity, reactive oxygen species production, and stability of the different samples were studied. The dissolution rate of all combinations was significantly increased in comparison to that of the pure active pharmaceutical ingredient. Additionally, oxidative stress production in human leukocytes caused by chloramphenicol was decreased in the chloramphenicol/amino acid combinations, while the antimicrobial activity of the antibiotic was maintained. The CAP:Leu binary combination resulted in the most outstanding solid system makes it suitable candidate for the development of pharmaceutical formulations of this antimicrobial agent with an improved safety profile.

KEY WORDS: dissolution; oxidative stress; solid-state NMR; physical stability; X-ray diffractometry.

INTRODUCTION

Recently, bacterial infections have become a major health problem. The advance of antimicrobial resistance required the introduction of new antibiotic compounds to treat infections caused by multidrug-resistant pathogens, but current research does not anticipate the presence of a promising active pharmaceutical ingredient (API) in the near future (1). Therefore, old antibiotics that had fallen into disuse have been applied to treat multidrug-resistant bacteria until new antibiotics are developed. In this context, chloramphenicol (CAP, Fig. 1a), an antibiotic with broad antibacterial activity (2,3), is re-emerging as a valuable alternative for the treatment of difficult-to-treat infections (4). In the past, serious side effects restricted the successful use of this API (5,6). Furthermore, CAP is a hydrophobic API, which exhibits poor solubility and dissolution rate in aqueous solution and therefore limits its clinical application. Some of the main factors that influence the kinetics of solubilization of an API are crystal habit, crystal size distribution, and the existence of polymorphs. There are several approaches to improve solubility and dissolution rate of poorly water-soluble APIs. Examples for the single-component systems include particle size reduction (7,8), polymorph selection, and the transfer of a crystalline API to its amorphous counterpart. For the multiple-component systems, we can mention salt or cocrystal formation (9–11), cyclodextrin complexation (12,13), amorphization [e.g., coamorphous systems (14–16)], and molecular dispersions in polymer carriers (17,18). In addition, by specifically selecting the auxiliary substance added (coformer or complexing agent), it is possible to reduce other problematic behaviors of the APIs, such as their toxicological properties.

In previous works, we have demonstrated the capacity of CAP to form multicomponent complexes with cyclodextrin and amino acids which allowed increasing its solubility and decreasing its toxic effects by modulating the production of

Electronic supplementary material The online version of this article (doi:10.1208/s12249-017-0775-4) contains supplementary material, which is available to authorized users.

[1] Unidad de Investigación y Desarrollo en Tecnología Farmacéutica (UNITEFA, CONICET) and Facultad de Ciencias Químicas, Universidad Nacional de Córdoba, Córdoba, Argentina.
[2] Instituto de Física Enrique Gaviola (IFEG, CONICET) and Facultad de Matemática, Astronomía y Física, Universidad Nacional de Córdoba, Córdoba, Argentina.
[3] To whom correspondence should be addressed. (e-mail: ariana@fcq.unc.edu.ar)

Published online: 20 April 2017

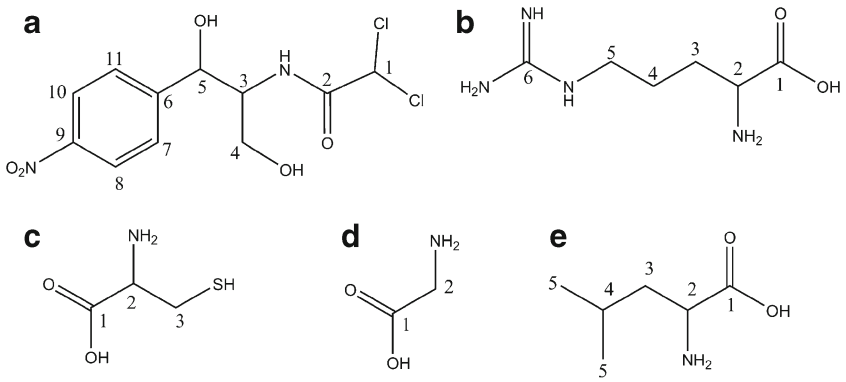

Fig. 1. Molecular structure and numbering scheme of carbon atoms. **a** CAP. **b** Arg. **c** Cys. **d** Gly. **e** Leu

oxidative stress (19,20). In these systems, CAP is in an amorphous state. Herein, we report our results on the preparation and characterization of two-component solid samples consisting of CAP and the amino acids arginine (Arg), cysteine (Cys), glycine (Gly), and leucine (Leu) (Fig. 1b–d) in which the API remains in its crystalline form. CAP and amino acid combinations were obtained using freeze-drying method, and the resulting solid materials were characterized by Fourier transform infrared spectroscopy (FTIR), powder X-ray diffraction (PXRD), differential scanning calorimetry (DSC), scanning electron microscope (SEM), and solid-state nuclear magnetic resonance (ssNMR) spectroscopy. In addition, the dissolution rate, antimicrobial activity, and potential toxic effects of pure CAP and solid binary combinations on human leukocytes were investigated. Finally, the physical stability of these binary combinations was also studied.

MATERIALS AND METHODS

Materials

CAP and Gly were obtained from Parafarm (Argentina). Cys, Arg, Leu, Ficoll-Hypaque (Histopaque-1077), dextran, and dihydrorhodamine 123 were purchased from Sigma-Aldrich (Milwaukee, WI, USA). All other materials and solvents were of analytical reagent grade. The water used in this investigation was produced by a Milli-Q Water Purification System (Millipore, USA).

Preparation of CAP:AA Solid Samples

Binary combinations ($CAP:AA_{BC}$ where AA is Arg, Cys, Gly, or Leu) were prepared by the freeze-drying method. Solutions of CAP and each AA (1:1 M ratio) were prepared in distilled water and sonicated in an ultrasonic bath at 25.0 ± 0.1°C for 1 h. Then, the solutions were frozen at 233 K before starting the freeze-drying process (Freeze Dryer 4.5, Labconco Corp., Kansas City, MI).

Physical mixture ($CAP:AA_{PM}$) was prepared by uniformly mixing in a mortar CAP and each AA with 1:1 M ratio.

Characterization of CAP:AA Solid Samples

Fourier Transform Infrared Spectroscopy

Spectra were recorded using a Nicolet Avatar 360 FTIR spectrometer. Acquisition was performed with the application of 40 scans at a resolution of 8 cm^{-1} over the range 4000–400 cm^{-1}. Each sample was prepared by mixing 1% (*w*/*w*) of API in potassium bromide (KBr).

Powder X-ray Diffraction

PXRD measurements were performed on a Philips X'Pert PRO PAN analytical powder diffractometer (Philips®, The Netherlands), using Ni-filtered CuKα radiation over the interval 5–40°/2θ, operating at 45 kW and 30 mA. The diffractograms were recorded with a step size of 0.02° and a scan step time of 2 s.

Differential Scanning Calorimetry

DSC experiments were carried out with a TA DSC Discovery series device. The samples (~1 mg) were weighed in an aluminum-pinhole pans and scanned from 30 to 170°C at a heating rate of 10°C min^{-1} under N_2 atmosphere (50 ml min^{-1}).

Scanning Electron Microscopy Studies

The morphology of samples was studied with a field emission scanning electron microscope (Carl Zeiss Σigma) at the Laboratorio de Microscopía y Análisis por Rayos X (LAMARX) of the National University of Córdoba. To carry out the SEM measurement, samples were mounted on metal stubs with double-sided adhesive tape and coated with gold/palladium employing a sputter coater Quorum 150 in order to make them conductive.

Solid-State Nuclear Magnetic Resonance

ssNMR was used to characterize the binary combinations and to evaluate possible solid-phase transformations under storage. High-resolution solid-state ^{13}C spectra were recorded using the ramp cross-polarization magic angle spinning (CPMAS) sequence with proton decoupling during acquisition (21). Solid-state ^{13}C spectra of pure CAP, Arg, Cys, Gly,

Preparation of Chloramphenicol/Amino Acid

and Leu; the binary combinations (CAP:AA_{BC}); and the corresponding physical mixtures (CAP:AA_{PM}) were recorded at the preparation time (T_0). In addition, the ^{13}C spectra of CAP:AA_{BC} were obtained after 1 month of storage (T_1) at 40°C/75% relative humidity (RH). All ssNMR experiments were performed at room temperature in a Bruker Avance II spectrometer operating at 300.13 MHz proton Larmor frequency, equipped with a 4-mm MAS probe. The operating frequency for carbons was 75.46 MHz. Glycine was used as an external reference for the ^{13}C spectra and for setting the Hartmann–Hahn matching condition in the cross-polarization experiments. The spectra were recorded with 1600 scans, a contact time of 2 ms during cross-polarization, and a recycling time of 5 s. The spinning rate for all the samples was 10 kHz.

Quaternary carbon edition spectrum was recorded for CAP at 10 kHz. This spectrum was acquired with the non-quaternary suppression (NQS) sequence, where the ^{1}H and ^{13}C radiofrequency fields are removed during 40 μs after cross-polarization and before acquisition. This delay allows the carbon magnetization to decay because of the ^{1}H–^{13}C dipolar coupling, which results in spectra where CH and CH_2 are substantially removed.

Dissolution Studies

The dissolution rate studies of pure CAP and CAP in all binary combinations were conducted in a dissolution apparatus (Hanson SRII 6 Flask Dissolution Test Station, Hanson Research Corporation, Chatsworth, USA) using the paddle method, according to USP XXX (22). One hundred milligrams of CAP or its equivalent amount of CAP:AA_{BC} was added to 900 ml of dissolution medium (diluted hydrochloric acid 0.1 N), maintained at 37.0 ± 0.5°C, and stirred at 100 rpm. Aliquots of 2 ml were taken at suitable time intervals, and the withdrawn samples were replaced with equal volumes of the fresh dissolution medium maintained at the same temperature. The cumulative percentage of the CAP released was determined spectrophotometrically (Shimadzu UV-Mini 1240 spectrophotometer) at 278 nm. The dissolution assay was evaluated in triplicate. The parameters used to compare the dissolution curves were the difference factor (f_1) (Eq. 1) and the similarity factor (f_2) (Eq. 2) (23):

$$f_1 = \frac{\sum_{t-1}^{R} |R_t - T_t|}{\sum R_t} \times 100 \quad (1)$$

$$f_2 = 50 \log \left\{ \left[1 + \frac{1}{n} \sum_{t-1}^{R} (R_t - T_t)^2 \right]^{-0,5} \right\} \times 100 \quad (2)$$

where n is the number of time points, R_t is the dissolution value of the reference (pure CAP), and T_t is the dissolution value of the test product (CAP:AA_{BC}) at time t.

Antimicrobial Activity Assay

Antimicrobial susceptibility tests were performed according to Zuorro *et al.* (24) with some modifications. Briefly, American Type Culture Collection (ATCC®) bacterial cells of *Escherichia coli* 25922 or *Staphylococcus aureus* 25923 from an exponential-phase culture obtained from a single colony were spread on the surface of agar Mueller Hinton plates using a sterile swab soaked in the bacterial suspension diluted to 10^6 colony forming units per milliliter (CFU ml^{-1}). A disk of 6 mm of sterile Whatman No. 1 membrane filters resting on an agar culture medium was inoculated with 10 μl of a solution containing pure or binary combinations of CAP (30 μg). Aqueous solutions of pure Arg, Cys, Gly, and Leu were used as a placebo control. After overnight incubation was performed at 37°C, the plates were examined and the diameters of the inhibition zones were measured. Measurements were made in triplicate, and the results were averaged.

ROS Analysis

For ROS analysis, peripheral blood samples were obtained during the same morning at 10 a.m. and placed into 20-ml syringes with heparin. Leukocytes were isolated by combined dextran (Sigma, average MW = 78.000)/Ficoll-Hypaque (Histopaque-1077, Sigma) sedimentation procedure (19). The isolated leukocytes were diluted in Hanks' balanced salt solution to a final concentration of 10^6 ml^{-1}. Leukocyte ROS was determined by the formation of the fluorescent compound rhodamine-123 from dihydrorhodamine-123 (DHR-123). Sixty microliter samples of leukocyte suspensions were incubated with 60 μl CAP solution (100 μg ml^{-1}), its binary combinations, or Hanks' buffer (control); 60 μl Hanks' buffer; and 20 μl DHR. ROS production was measured by means of the fluorescence intensity technique (excitation, 428–20 nm; emission, 528–20 nm; gain, 50) in BioTek Microplate Readers.

Stability Studies of CAP:AA_{BC}

The binary combinations were kept in a tightly sealed container under accelerated storage conditions (40°C/75% RH) and examined after 1 month of storage. The physical stability of the samples was analyzed by ssNMR and SEM in order to investigate possible solid transformations. Additionally, to check whether the microbiological activity was kept, the samples were tested after 1 month of storage as described in Section Antimicrobial Activity Assay.

RESULTS AND DISCUSSION

Characterization of CAP:AA Solid Samples

FTIR, PXRD, DSC, and SEM

In order to identify possible molecular interactions, changes in solid-state forms, and morphology of the samples, FTIR, PXRD, DSC and SEM analysis were carried out.

In all FTIR spectra of CAP:AA_{BC} (Fig. 2), it was possible to observe the fundamental bands of CAP at 3347 cm^{-1} (ν_{OH}), 3262 cm^{-1} (ν_{NH}), 3079 cm^{-1} (δ_{NH}), 2962 cm^{-1} (ν_{CH2}), 1687 cm^{-1} ($\nu_{C=O}$), 1559 cm^{-1} (δ_{NH}), and 1526 cm^{-1} ($\nu_{N=O2}$). The absence of significant changes in the

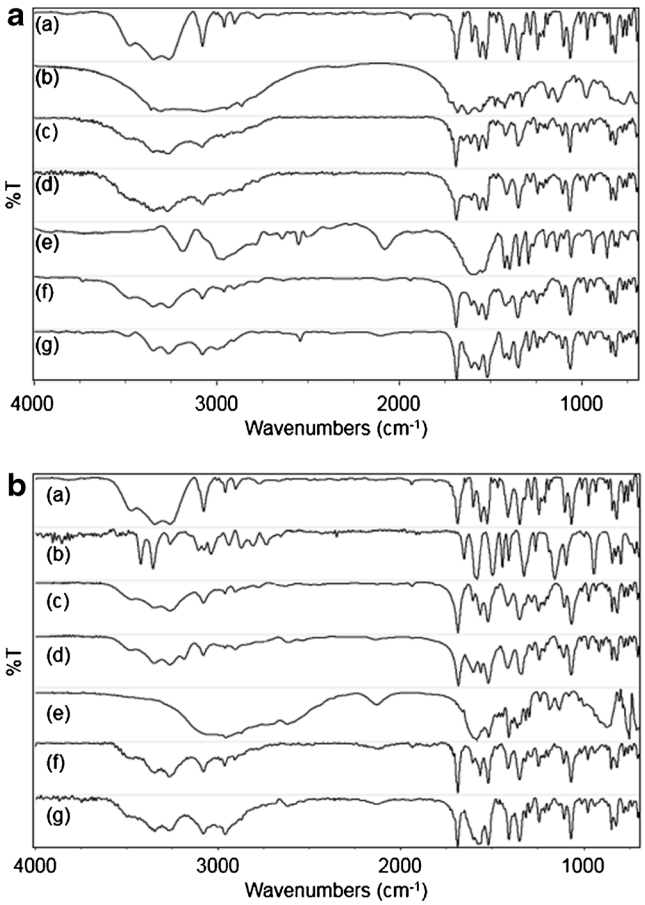

Fig. 2. IR spectra of **a** CAP (*a*), Arg (*b*), CAP:Arg_{PM} (*c*), CAP:Arg_{BC} (*d*), Cys (*e*), CAP:Cys_{PM} (*f*), and CAP:Cys_{BC} (*g*) and **b** CAP (*a*), Gly (*b*), CAP:Gly_{PM} (*c*), CAP:Gly_{BC} (*d*), Leu (*e*), CAP:Leu_{PM} (*f*), and CAP:Leu_{BC} (*g*)

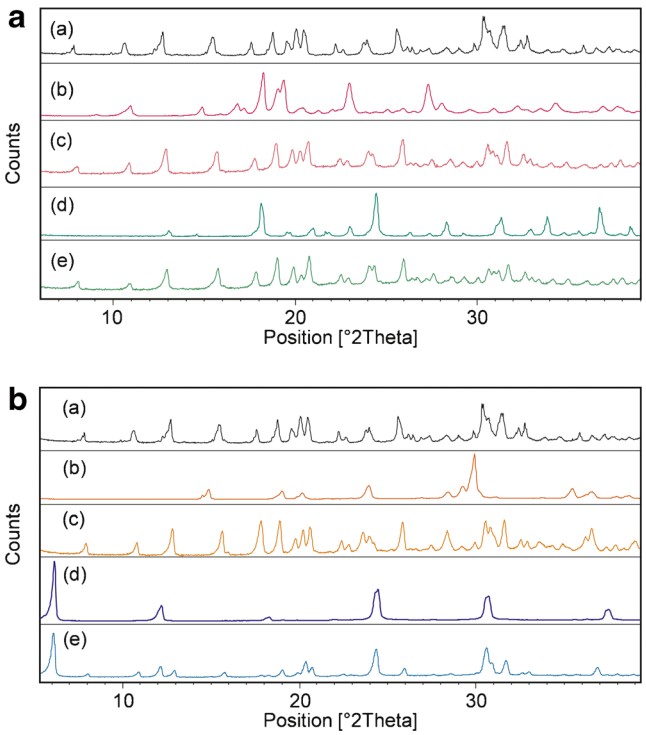

Fig. 3. X-ray diffractograms of **a** CAP (*a*), Arg (*b*), CAP:Arg_{BC} (*c*), Cys (*d*), and CAP:Cys_{BC} (*e*) and **b** CAP (*a*), Gly (*b*), CAP:Gly_{BC} (*c*), Leu (*d*), and CAP:Leu_{BC} (*e*)

bands of API suggested that there were no important interactions between CAP and the different AAs.

The PXRD patterns of the untreated CAP and the different combinations with AAs (see Fig. 3) exhibited essentially similar diffraction patterns than that of CAP, suggesting that the drug particles obtained in the presence of each AA did not undergo structural modifications. In addition, it was possible to observe differences in the relative intensities of the peaks of CAP, which may be due to changes in the crystal sizes and habits of the solid products. On the other hand, the binary combinations obtained with Arg, Cys, and Gly exhibited a decrease in the AA degree of crystallinity.

Figure 4a, b shows the DSC thermograms of pure CAP, pure amino acids, and the corresponding CAP:AA_{BC} samples. The melting endotherm of CAP (150.8°C) was well preserved in the majority of the binary combinations (CAP:Cys_{BC} 149.6°C, CAP:Gly_{BC} 150.1°C, and CAP:Leu_{BC} 149.9°C). However, there were slight changes in the peak shape in which a slight broadening was observed. These results evidence that physical interactions of components did not occur within these CAP:AA_{BC} samples. On the other hand, in the thermogram corresponding to CAP:Arg_{BC}, significant downward shift of the CAP peak temperature (137.7°C) was found, which can be indicative of some kind of drug/amino acid interaction.

The SEM images showed clear differences in the crystal habit of CAP in all CAP:AA_{BC} with respect to pure CAP (Fig. 5). In all CAP:AA_{BC}, it was possible to observe acicular hollow crystals of CAP with a smaller particle size than that of pure API.

ssNMR

Figure 6 displays the high-resolution solid-state ^{13}C (CP-MAS) spectra of pure CAP, Arg, Cys, Gly, and Leu. Carbon numbering of each molecule is shown in Fig. 1. Supplemental Tables 1–4 of supporting information show the corresponding chemical shifts for API, each AA, physical mixtures, and binary combinations.

The assignments of CAP spectrum were performed taking into account the NQS spectrum and the ^{13}C solid-state spectrum of CAP reported by Zolek *et al.* (25). The assignments for the AAs were carried out considering the data available in the literature (26,27). It is interesting to note that the ^{13}C spectra of all AAs revealed a high degree of crystallinity.

Figure 7 displays the comparison between the physical mixture and the binary combination of CAP and each AA at time T_0. In the physical mixture spectra, the signals corresponding to the AA were distinguished from those of CAP with circled numbers in order to follow possible changes.

For all the AAs, the physical mixtures of ^{13}C spectra were the superposition of the individual spectra for each component (CAP and the corresponding AA), which evidenced that there was no interaction during the mixture. On other hand, when comparing the ^{13}C solid-state NMR spectra of each physical mixture with those of the

Preparation of Chloramphenicol/Amino Acid

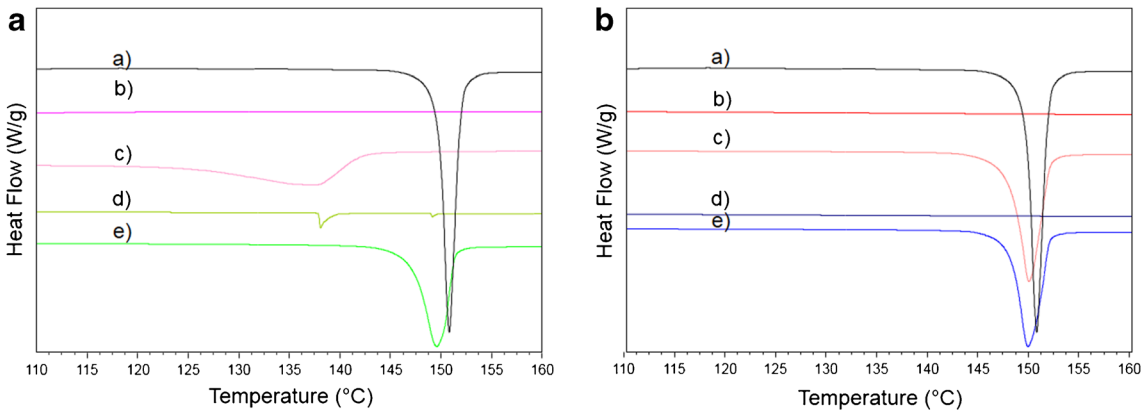

Fig. 4. DSC thermograms of **a** CAP (*a*), Arg (*b*), CAP:Arg_{BC} (*c*), Cys (*d*), and CAP:Cys_{BC} (*e*) and **b** CAP (*a*), Gly (*b*), CAP:Gly_{BC} (*c*), Leu (*d*), and CAP:Leu_{BC} (*e*)

corresponding binary combination at T_0, it was possible to extract information involving possible modifications of the structures of both CAP and AAs.

The ^{13}C ssNMR spectrum of CAP:Arg_{BC} differed notably from that of CAP:Arg_{PM}. The resonance signals belonging to Arg became distinctly wider in the binary combination (from 80 to 250 Hz). Also, a change in the chemical shift of the resonance lines of the Arg was observed (see, for example, the signal corresponding to carbon C_5). In contrast, the CAP signals of the binary combination did not evidence broadening or changes in the chemical shifts.

The same behavior was observed in CAP:Cys_{BC}. The line width of Cys signals increased (approximately 50 Hz), and changes in the chemical shifts of the signals corresponding to this AA were observed. An interesting observation was the splitting in some of the resonance lines of Cys (e.g., the signal corresponding to C_1), leading to the conclusion that a change in the molecular structure of Cys took place upon the combination preparation. Note that the signals corresponding to CAP did not present variations in the chemical shifts or line width in the binary combination, which demonstrated that this API did not change its solid-state structure.

The ^{13}C ssNMR spectrum of CAP:Gly_{PM} was similar to that of CAP:Gly_{BC}. As noted above for the other combinations, the chemical shifts of the resonance lines of CAP did not present variations (see supplemental Table 3). Again, the signals more affected in the line width were those corresponding to the AA. Gly signals became slightly wider. Moreover, a splitting in the resonance lines was observed, indicating a change in the structure of the AA after obtaining the binary combination. The last combination studied showed that the ^{13}C ssNMR spectrum of CAP-Leu_{PM} and that of CAP-Leu_{BC} were similar. The chemical shifts did not present any variation (see supplemental Table 4). Furthermore, note that carbon signals of Leu in the binary combination became slightly wider (20 Hz).

From the above, we can conclude that while CAP maintained its structure, the AAs showed modification in their molecular structures after combination preparation. In all cases,

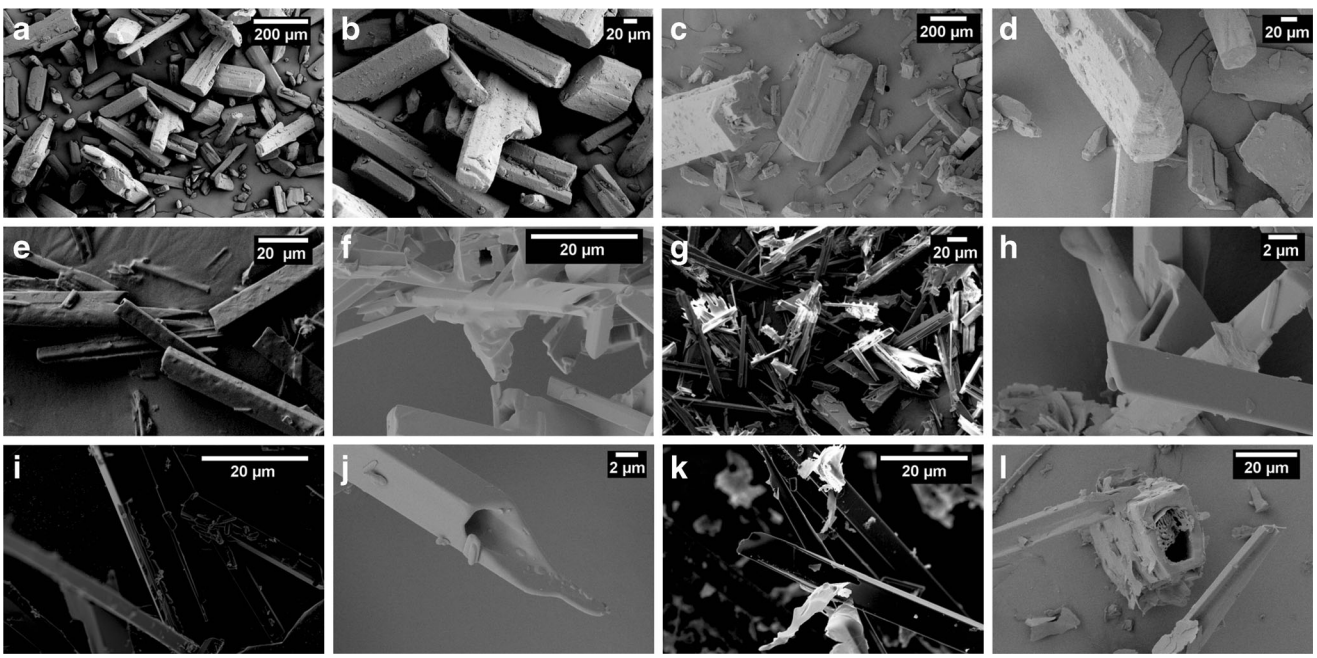

Fig. 5. Scanning electron microphotographs of **a**, **b** CAP T_0, **c**, **d** CAP T_1, **e** CAP:Arg_{BC} T_0, **f** CAP:Arg_{BC} T_1, **g** CAP:Cys_{BC} T_0, **h** CAP:Cys_{BC} T_1, **i** CAP:Gly_{BC} T_0, **j** CAP:Gly_{BC} T_1, **k** CAP:Leu_{BC} T_0, and **l** CAP:Leu_{BC} T_1

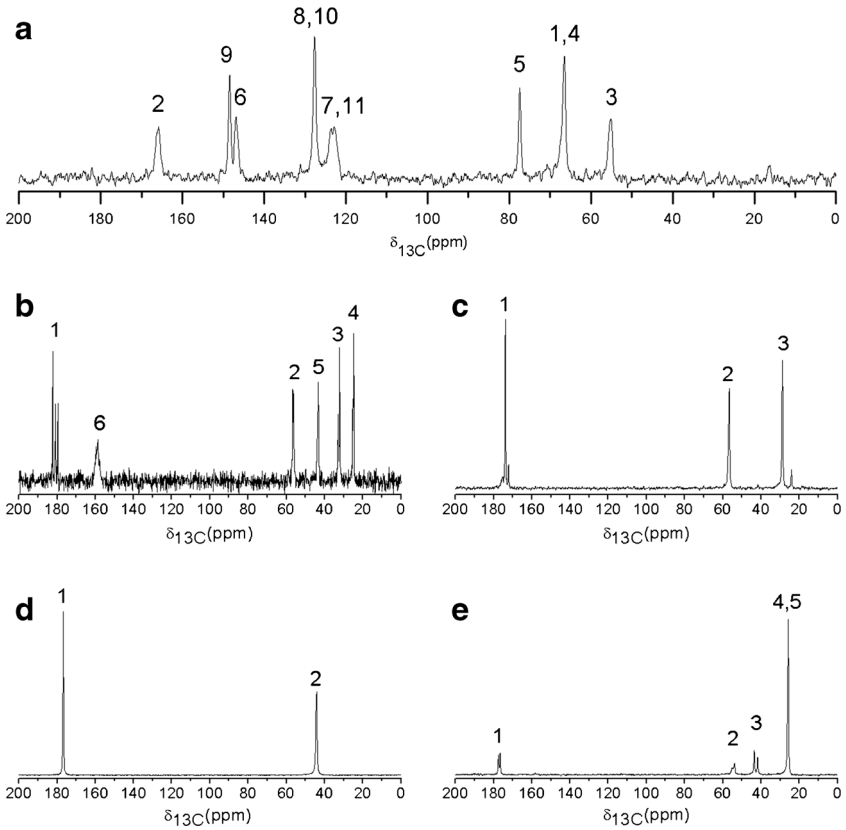

Fig. 6. Solid-state ^{13}C CP/MAS NMR spectra of **a** CAP, **b** Arg, **c** Cys, **d** Gly, and **e** Leu

the widening observed in the peaks corresponding to the AAs can be attributed to a decrease in the degree of crystallinity of the AAs, probably due to the freeze-drying process.

The results of FTIR, PXRD, DSC, SEM, and ssNMR studies showed that there were no evident intermolecular interactions between CAP and each AA. In addition, a decrease in the degree of crystallinity of the different AAs was observed. Finally, the crystal structure of CAP was not modified, although a drastic change in its crystalline habit was identified. This fact may lead to a modification of its dissolution rate.

Dissolution Studies

The dissolution profiles of pure CAP and CAP:AA_{BC} are shown in Fig. 8. The percentage of API dissolved within 10 min was increased in all CAP:AA_{BC} (CAP:Arg 98 ± 3%; CAP:Cys 66 ± 5%; CAP:Gly 73 ± 7%; CAP:Leu 97 ± 1%) with respect to that of pure API (55 ± 1%). To compare the dissolution profiles of CAP:AA_{BC} with that of pure CAP, the difference factor (f_1) and the similarity factor (f_2) were calculated. The f_1 and f_2 values obtained were 42 and 27 (CAP:Arg), 20 and 43 (CAP:Cys), 24 and 39 (CAP:Gly), and 42 and 27 (CAP:Leu), respectively. In general, f_1 value lower than 15 (0–15) and f_2 value higher than 50 (50–100) indicated the similarity of the two dissolution profiles.

In all cases, f_1 and f_2 values were higher than 15 and lower than 50, respectively, thus indicating that the dissolution profiles of all combinations were different from those of pure CAP. These results demonstrated that CAP:AA_{BC} exhibited improved dissolution rate compared to that of the pure antimicrobial agent. This feature could be derived from the changes in the crystal habit of CAP and the reduction of its particle size. Also, additional factors, such as an increase in the system wettability, may also contribute to the overall increase in the dissolution rate.

Antimicrobial Activity Assay

The antimicrobial activity of CAP:AA_{BC} against *S. aureus* and *E. coli* was investigated by the agar diffusion methods and compared with that of pure CAP. In the same test, it was observed that pure Arg, Cys, Gly, and Leu did not exhibit antimicrobial activity against these species. The antimicrobial activity assays showed that there were no significant differences between the inhibition zones of pure CAP and the binary combinations of the species under study (Table I). These results indicated that these combinations containing CAP and AA, in which API remains in crystalline form, did not interfere with the microbiological activity of CAP. Therefore, it was inferred that the presence of each AA was enough to enhance the solubility of CAP in an aqueous environment without exerting detrimental effects on its *in vitro* activity against the bacterial species under study.

ROS Analysis

Research on the toxicology of CAP indicates that its propensity to cause damage to the blood-forming organs could be related to its potential for nitro-reduction and subsequent production of nitric oxide. These observations suggest that the para-nitro group of CAP could be the cause of hemotoxicity in susceptible people (28). The results obtained by Eraso and Albesa (29) showed that blood cells

Preparation of Chloramphenicol/Amino Acid

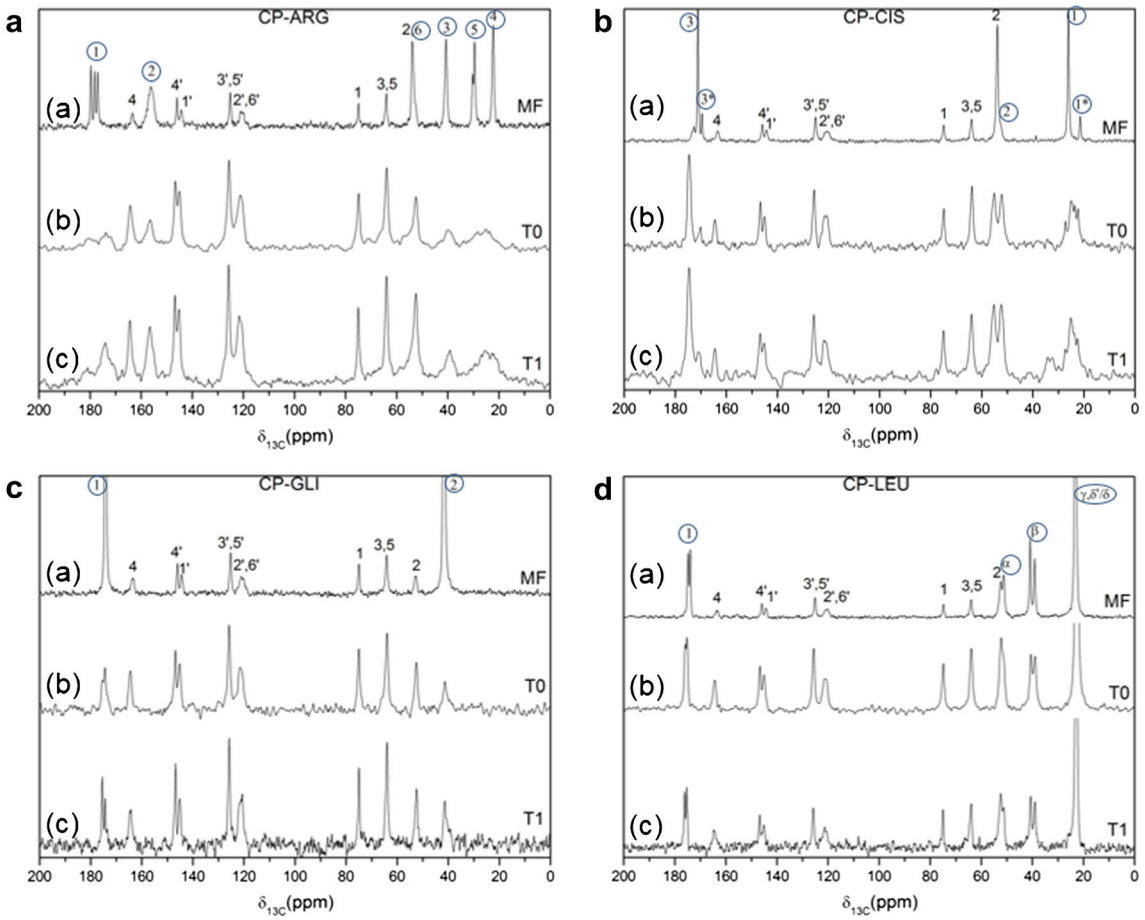

Fig. 7. Solid-state ^{13}C CP/MAS NMR spectra of **a** CAP:Arg_{PM} (*a*), CAP:Arg_{BC} T_0 (*b*), and CAP:Arg_{BC} T_1 (*c*); **b** CAP:Cys_{PM} (*a*), CAP:Cys_{BC} T_0 (*b*), and CAP:Cys_{BC} T_1 (*c*); **c** CAP:Gly_{PM} (*a*), CAP:Gly_{BC} T_0 (*b*), and CAP:Gly_{BC} T_1 (*c*); **d** CAP:Leu_{PM} (*a*), CAP:Leu_{BC} T_0 (*b*), and CAP:Leu_{BC} T_1 (*c*). The signals corresponding to the AA were distinguished from those of CAP with *circled numbers*

suffer oxidative stress in the presence of CAP since it causes a significant increase in ROS, which can be detected by luminol chemiluminescence (CL). This increase in ROS can be markedly decreased with the extract of fruits of *Eriobotrya japonica* associated with the action of vitamin A. Antioxidants can be employed to prevent the generation of ROS, destroy potential oxidants, and scavenge ROS. Thus, oxidative stress-induced cell and tissue damages are minimized (30). Based on this background, it was interesting to assess the effect of the presence of Arg, Cys, Gly, or Leu combined with CAP on leukocyte ROS production.

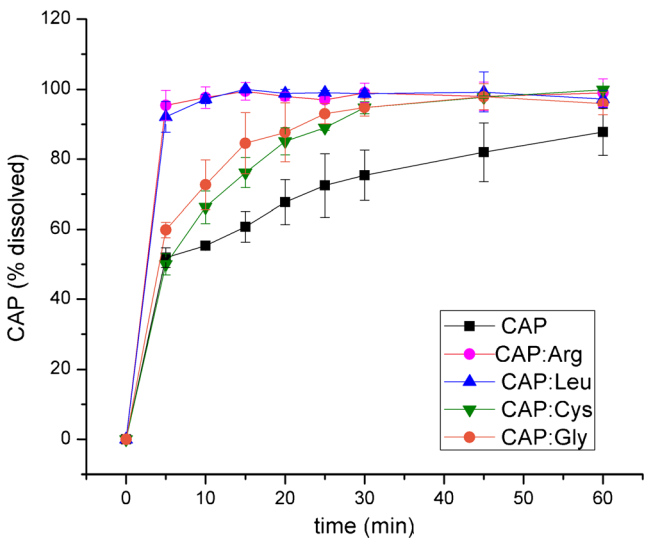

Fig. 8. Dissolution rate profiles for CAP, CAP:Arg_{BC}, CAP:Cys_{BC}, CAP:Gly_{BC}, and CAP:Leu_{BC}

When the binary combinations were assayed, it was observed that the levels of ROS were significantly lower than those of the samples treated with pure CAP (Fig. 9), suggesting that the AAs worked as ROS inhibitor/scavengers. In fact, it is known that the cyclic oxidation and reduction of the sulfur-containing amino acids may serve as an important antioxidant mechanism and that these reversible oxidations may provide an important mechanism for the regulation of some enzyme functions (31). These results have demonstrated that the binary combinations of CAP and each AA are useful to reduce the damaging effects of CAP without affecting its antimicrobial activity.

Table I. Antimicrobial Activity of Pure CAP and CAP:AA_{BC}

Systems	Zone size (mm)[a] mean ± SD			
	S. aureus 25923		*E. coli* 25922	
	T_0	T_1	T_0	T_1
CAP	27.5 ± 0.5	28 ± 1	30 ± 1	31 ± 1
CAP:Arg_{BC}	28.5 ± 0.5	28 ± 1	29.5 ± 0.5	30.5 ± 0.5
CAP:Cys_{BC}	27 ± 1	28 ± 1	31.5 ± 0.5	32 ± 1
CAP:Gly_{BC}	27.5 ± 0.5	29 ± 1	28.5 ± 0.5	30 ± 1
CAP:Leu_{BC}	27.5 ± 0.5	28 ± 1	28.5 ± 0.5	30 ± 1

SD standard deviation
[a] Mean of three experiments

Stability Studies of CP:AA_{BC}

Temperature and humidity are important factors responsible for the physical instability of APIs during normal storage conditions because they may promote the reorganization of molecules in the crystal. ssNMR provides a direct way to monitor phase changes under storage conditions (32). In this work, ssNMR and SEM were used to evaluate the physical stability of pure CAP and the different combinations containing AAs over 1 month of storage at 40°C/75% RH. In addition, the microbiological activity of these stored samples was analyzed.

When comparing SEM microphotographs and ssNMR spectra (Figs. 5 and 7, respectively) of the binary combinations obtained at the preparation time (T_0) and after 1 month of storage (T_1), it was possible to obtain information about the physical stability of the samples.

In CAP:Gly_{BC} and CAP:Leu_{BC} spectra, there were no important variations after 1 month of storage because the chemical shifts remained in the same positions and there was no disappearance of signals (see supplemental Tables 3 and 4, respectively). In CAP:Cys_{BC}, there were no major changes although slight variations could be seen for the C_1 resonance of Cys. It was the same for CAP:Arg_{BC}, where there were no major variations in the spectra although there were some changes in the signal width of Arg C_1, C_3, C_4, and C_5. It is important to clarify that these changes in the structure did not affect the properties of these binary combinations. In none of the four combinations studied were major changes observed in the chemical shifts of CAP after 1 month of storage.

In addition, SEM microphotographs revealed that the morphology of CAP was not altered during storage at 40°C/75% RH for 1 month, demonstrating the physical stability of CAP in all combinations.

Moreover, the antimicrobial activity of CAP did not show statistically significant differences when the combinations were assayed at T_0 and after being kept under accelerated storage conditions (see Table I). These results have demonstrated that CAP maintained not only its physical stability but also its microbiological activity in all the combinations studied.

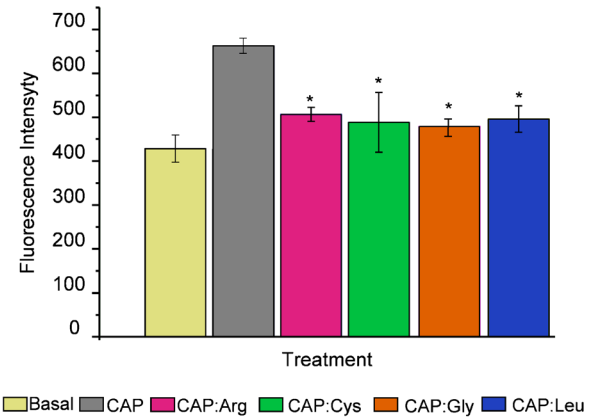

Fig. 9. Quantification of reactive oxygen species in human leukocytes by fluorescence assay. *$P < 0.05$, compared to the sample treated with CAP

CONCLUSIONS

In this article, we described the development and evaluation of the performance of chloramphenicol in combination with different amino acids prepared by the freeze-drying method in order to enhance the dissolution rate and decrease the oxidative stress produced by this API. The solid-state characterization results of FTIR, PXRD, DSC, SEM, and ssNMR showed that there were no marked intermolecular interactions between CAP and each AA in the binary combinations. In fact, although the crystal structure of CAP was not changed, a significant modification of its crystalline habit was observed. The CAP:AA binary combinations presented better dissolution rates than those of the pure API. In addition, the incorporation of each AA into these combinations allowed reducing the CAP levels of ROS production in human leukocytes, while the antimicrobial activity of this API was not modified.

Finally, the CAP:Leu binary combination resulted in the most outstanding solid system, since it exhibited the highest difference in its dissolution profile compared to that of pure CAP (f_1 42 and f_2 27). In relation to CAP:Arg_{BC} and despite the fact that it presented the same f_1 and f_2 values as CAP:Leu_{BC}, the DSC studies showed that CAP exhibited interaction with Arg that may compromise the stability of this binary combination. In addition, although the four combinations maintained their microbiological activity and physical properties after 1 month of storage at 40°C/75% RH, formulations with AA in the amorphous state may exhibit inadequate physical stability (crystallization) during storage. In this respect, the CAP:Leu_{BC} combination presents the advantage of exhibiting a crystalline state, which, in turn, constitutes a promising feature in light of its potential for the production of different dosage forms of CAP with better biopharmaceutical and safety profiles.

ACKNOWLEDGEMENTS

Authors wish to acknowledge the assistance of the Consejo Nacional de Investigaciones Científicas y Técnicas (CONICET) and the Universidad Nacional de Córdoba, both of which provided support and facilities for this investigation. This work was supported by the Fondo para la Investigación Científica y Tecnológica (FONCYT) [Préstamo BID PICT

2013-2150] and the Secretaría de Ciencia y Técnica de la Universidad Nacional de Córdoba (SECyT).

REFERENCES

1. Falagas ME, Grammatikos AP, Michalopoulos A. Potential of old-generation antibiotics to address current need for new antibiotics. Expert Rev Anti-Infe. 2008;6(5):593–600.
2. Stratton CW. Chloramphenicol. Antimicrob Infect Dis Newsl. 2002;18(12):89–91.
3. Sweetman SC, Blake PS. Martindale: the complete drug reference. 36th ed. London: Pharmaceutical Press; 2009.
4. Liaqat I, Sumbal F, Sabri AN. Tetracycline and chloramphenicol efficiency against selected biofilm forming bacteria. Curr Microbiol. 2009;59(2):212–20.
5. Moffa M, Brook I. 26 - Tetracyclines, glycylcyclines, and chloramphenicol. In: Bennett JE, Dolin R, Blaser MJ, editors. Mandell, Douglas, and Bennett′s Principles and Practice of. Infectious Diseases. 8th ed. Philadelphia: Saunders; 2015. p. 322–38.
6. Singh R, Sripada L, Singh R. Side effects of antibiotics during bacterial infection: mitochondria, the main target in host cell. Mitochondrion. 2014;16:50–4.
7. Rodríguez-Spong B. General principles of pharmaceutical solid polymorphism A supramolecular perspective. Adv Drug Deliv Rev. 2004;56(3):241–74.
8. Kawabata Y, Wada K, Nakatani M, Yamada S, Onoue S. Formulation design for poorly water-soluble drugs based on biopharmaceutics classification system: basic approaches and practical applications. Int J Pharm. 2011;420(1):1–10.
9. Aitipamula S, Banerjee R, Bansal AK, Biradha K, Cheney ML, Choudhury AR, et al. Polymorphs, salts, and cocrystals: what's in a name? Cryst Growth Des. 2012;12(5):2147–52.
10. Balk A, Wiest J, Widmer T, Galli B, Holzgrabe U, Meinel L. Transformation of acidic poorly water soluble drugs into ionic liquids. Eur J Pharm Biopharm. 2015;94:73–82.
11. Thakuria R, Delori A, Jones W, Lipert MP, Roy L, Rodríguez-Hornedo N. Pharmaceutical cocrystals and poorly soluble drugs. Int J Pharm. 2013;453(1):101–25.
12. Crini G. Review: a history of cyclodextrins. Chem Rev. 2014;114(21):10940–75.
13. Loftsson T, Brewster ME. Cyclodextrins as functional excipients: methods to enhance complexation efficiency. J Pharm Sci. 2012;101(9):3019–32.
14. Löbmann K, Grohganz H, Laitinen R, Strachan C, Rades T. Amino acids as co-amorphous stabilizers for poorly water soluble drugs—part 1: preparation, stability and dissolution enhancement. Eur J Pharm Biopharm. 2013;85(3, Part B):873–81.
15. Löbmann K, Laitinen R, Strachan C, Rades T, Grohganz H. Amino acids as co-amorphous stabilizers for poorly water-soluble drugs—part 2: molecular interactions. Eur J Pharm Biopharm. 2013;85(3, Part B):882–8.
16. Löbmann K, Strachan C, Grohganz H, Rades T, Korhonen O, Laitinen R. Co-amorphous simvastatin and glipizide combinations show improved physical stability without evidence of intermolecular interactions. Eur J Pharm Biopharm. 2012;81(1):159–69.
17. Grohganz H, Priemel PA, Löbmann K, Nielsen LH, Laitinen R, Mullertz A, et al. Refining stability and dissolution rate of amorphous drug formulations. Expert Opin Drug Del. 2014;11(6):977–89.
18. Kanaujia P, Poovizhi P, Ng WK, Tan RBH. Amorphous formulations for dissolution and bioavailability enhancement of poorly soluble APIs. Powder Technol. 2015;285:2–15.
19. Aiassa V, Zoppi A, Albesa I, Longhi MR. Inclusion complexes of chloramphenicol with β-cyclodextrin and aminoacids as a way to increase drug solubility and modulate ROS production. Carbohydr Polym. 2015;121:320–7.
20. Aiassa V, Zoppi A, Becerra MC, Albesa I, Longhi MR. Enhanced inhibition of bacterial biofilm formation and reduced leukocyte toxicity by chloramphenicol:β-cyclodextrin:N-acetylcysteine complex. Carbohydr Polym. 2016;152:672–8.
21. Harris RK. Nuclear magnetic resonance spectroscopy. London: Longman Scientific and Technical; 1994.
22. The United States Pharmacopeia (USP 30). Rockville, MD 2007.
23. US Department of Health and Human Services FaC. Guidance for industry. Dissolution testing of immediate release solid oral dosage forms. 1997.
24. Zuorro A, Fidaleo M, Lavecchia R. Solubility enhancement and antibacterial activity of chloramphenicol included in modified β-cyclodextrins. B Kor Chem Soc. 2010;31(11):3460–2.
25. Zołek T, Paradowska K, Krajewska D, Rózański A, Wawer I. 1H, 13C MAS NMR and GIAO-CPHF calculations of chloramphenicol, thiamphenicol and their pyrrole analogues. J Mol Struct. 2003;646(1–3):141–9.
26. Tadeusiak EJ, Ciesielski W, Olejniczak S. Determination of enantiomeric excess of leucine by 13C CP-MAS solid-state NMR. Appl Magn Reson. 2008;35(1):155–61.
27. Prakash S, Iturmendi N, Grelard A, Moine V, Dufourc E. Quantitative analysis of Bordeaux red wine precipitates by solid-state NMR: role of tartrates and polyphenols. Food Chem. 2016;199:229–37.
28. Holt DE, Bajoria R. The role of nitro-reduction and nitric oxide in the toxicity of chloramphenicol. Hum Exp Toxicol. 1999;18(2):111–8.
29. Eraso AJ, Albesa I. *Eriobotrya japonica* counteracts reactive oxygen species and nitric oxide stimulated by chloramphenicol. Am J Chin Med. 2007;35(5):875–85.
30. Gutteridge JMC. Lipid peroxidation and antioxidants as biomarkers of tissue damage. Clin Chem. 1995;41:1819–28.
31. Stadtman ER, Levine RL. Free radical-mediated oxidation of free amino acids and amino acid residues in proteins. Amino Acids. 2003;25(3):207–18.
32. Monti GA, Chattah AK, Linck YG. Solid-state nuclear magnetic resonance in pharmaceutical compounds. Ann R NMR S. 2014. p. 221–69.